Published in final edited form as:

Neuron. 2017 May 17; 94(4): 920–930.e3. doi:10.1016/j.neuron.2017.04.033.

Indirect pathway of caudal basal ganglia for rejection of valueless visual objects

Hyoung F. Kim[1,2], **Hidetoshi Amita**[3], and **Okihide Hikosaka**[3,4]

[1]Department of Biomedical Engineering, Sungkyunkwan University (SKKU), Suwon 16419, Republic of Korea

[2]Center for Neuroscience Imaging Research, Institute for Basic Science (IBS), Suwon 16419, Republic of Korea

[3]Laboratory of Sensorimotor Research, National Eye Institute, National Institutes of Health Bethesda, Bethesda, MD, USA

[4]National Institute on Drug Abuse, National Institutes of Health, Bethesda, MD, USA

Summary

The striatum controls behavior in two ways: facilitation and suppression through the direct and indirect pathways respectively. However, it is still unclear what information is processed in these pathways. To address this question, we studied two pathways originating from the primate caudate tail (CDt). We found that the CDt innervated the caudal-dorsal-lateral part of the substantia nigra pars reticulata (cdlSNr), directly or indirectly through the caudal-ventral part of the globus pallidus externus (cvGPe). Notably, cvGPe neurons receiving inputs from the CDt were mostly visual neurons that encoded stable reward values of visual objects based on long-past experiences. Their dominant response was inhibition by valueless objects, which generated disinhibition of cdlSNr neurons and inhibition of superior colliculus neurons. Our data suggest that low-value signals are sent by the CDt-indirect pathway to suppress saccades to valueless objects, whereas high-value signals are sent by the CDt-direct pathway to facilitate saccades to valuable objects.

Introduction

The basal ganglia contribute to motor planning and execution in various contexts (Marsden, 1982). Critical for these functions are the direct and indirect pathways which, together, are fundamental to the circuit mechanisms of the basal ganglia (Alexander and Crutcher, 1990;

Corresponding author and lead contact: Hyoung F. Kim hyoung.f.kim@gmail.com.

AUTHOR CONTRIBUTIONS

H.F.K and O.H. designed the research; H.F.K and H.A. analyzed the data; H.F.K and H.A. performed the research; H.F.K and O.H. wrote the paper.

Additional Information

We declare that there is no conflict of interest regarding the publication of this article.

Lévesque and Parent, 2005; Smith et al., 1998). According to a simplified scheme (Hikosaka et al., 2000), the direct and indirect pathways work separately and provide opposite effects. Indeed, recent studies have shown that body movements are facilitated and suppressed by the direct and indirect pathways in the basal ganglia, respectively (Kravitz et al., 2010; Roseberry et al., 2016). On the other hand, both of these pathways may become active during natural behaviors (e.g., contraversive movement) (Cui et al., 2013).

These studies are critical for understanding the output functions of the basal ganglia. However, their input functions are still unclear: what kinds of information activate (or inhibit) the direct and indirect pathways? It has been suggested that the basal ganglia contribute to decision making based on reward values (O'Doherty et al., 2004; Samejima et al., 2005; Schultz et al., 1997), with the direct and indirect pathways playing different roles (Hikida et al., 2010; Kravitz et al., 2012; Tai et al., 2012). However, it is unknown how the value information is processed through the direct and indirect pathways.

To address this question, we chose saccadic eye movements, which are well known to be controlled by the basal ganglia, CD-SNr-SC circuit (i.e., CD: caudate nucleus, SNr: substantia nigra par reticulata, SC: superior colliculus) (Hikosaka et al., 2000). Recently we found that the caudal (i.e., tail) region of CD-SNr-SC circuit in macaque monkeys processes reward values of visual objects stably to control saccades automatically, choosing high-valued (good) objects and rejecting low-valued (bad) objects (Hikosaka et al., 2014; Kim and Hikosaka, 2013). We thus hypothesized that the direct and indirect pathways originating from CDt guide the selection and rejection of saccades according to the object values.

To test this hypothesis, we mainly investigated the CDt-indirect pathway, especially the connection and function of the globus pallidus external segment (GPe). This is critical because there has been no study, to our knowledge, on the function of the indirect pathway in primates. Here we show anatomical and functional connections of the CDt-originated indirect pathway and its selective value processing for automatic saccades.

Results

Caudal-ventral GPe is a key station of CDt-originating indirect pathway

To examine the indirect pathway originating from CDt, we injected two anatomical tracers in CDt: alexa488- and alexa555-conjuated cholera toxin subunit B (CTB488 and CTB555) in the anterior and posterior regions of CDt (Fig. 1A and B). We used injectrodes to inject the tracers accurately in CDt. Before each injection, we recorded neuronal activity that encoded stable values of visual objects (Kim and Hikosaka, 2013; Yamamoto et al., 2013), thus confirming that the tracer would be injected inside CDt.

We found anterogradely labeled axon terminals in ventral regions of GPe (Fig. 1C and E). Coronal sections in the rostral-caudal axis indicate that labeled axon terminals were localized in the caudal-ventral region of GPe (Fig. 1D). Notably, the anterior region of CDt, compared with the posterior region of CDt, projected to the slightly more anterior region of GPe (Fig. 1F). Overall, indirect pathway neurons in CDt projected selectively to the caudal-

ventral region of GPe (cvGPe) (Fig. 1F and S1A,B,D), indicating that cvGPe is a key station of CDt-originating indirect pathway.

Visual neurons in GPe

Since CDt neurons are visually responsive and show clear spatial and object selectivity, cvGPe neurons may have similar responsive properties. We first tested neurons in all regions of GPe to examine their visual responsiveness (Fig. 2A, top); 212 out of 539 neurons showed visual responses to fractal objects during passive viewing. These visual neurons were more abundant in the caudal-ventral region of GPe (Fig. 2A), which is likely to include the CDt-recipient area: cvGPe.

Some of these visual neurons responded more strongly to fractal objects presented in the contralateral field than ipsilateral field (Fig. 2B–D). To test their visual response properties, we presented one fractal object (which caused strong responses in the neuron) at different positions during the passive viewing task (Fig. 2B, left). Since all output neurons in the striatum (including CDt) are thought to be GABAergic and inhibitory (Graybiel, 1990; Kita, 1993; Yoshida and Precht, 1971), we predicted that the visual responses of GPe neurons would be inhibitory. An example neuron indeed showed inhibitory responses (Fig. 2B, right). Notably, the inhibitory response was restricted to the contralateral side. This was also expected, because most CDt neurons had contralateral receptive fields (Yamamoto et al., 2012).

Although the inhibitory response was more common (n=20) (Fig. 2C and D, left), some GPe neurons (n=9) showed excitatory visual responses (Fig. 2D, right). Many of the visual neurons, either inhibitory or excitatory, showed significantly stronger responses to the contralateral than ipsilateral field (15 out of 29, 52%) ($p < 0.05$, Wilcoxon rank-sum test); no neurons showed ipsilateral preference (Fig. 2C). These data suggest that many of the GPe neurons receive visual-spatial signals from CDt.

We next compared electrophysiological properties of visual neurons and non-visual neurons recorded in GPe. The two groups were very similar in spike shape (Fig. 2E) and baseline activity (non-visual: 73.0 ± 30.0 Hz; visual: 70.1 ± 27.4 Hz, mean ± SD) (Fig. 2F).

However, visual neurons tended to fire more regularly than non-visual neurons (non-visual: 0.60 ± 0.18; visual: 0.54 ± 0.17, mean ± SD) ($p < 0.05$, Wilcoxon rank-sum test) (Fig. 2G).

Reward value coding in GPe neurons

If visual neurons in GPe receive inputs from CDt, they may encode reward values of visual objects stably, similarly to CDt. To test this hypothesis, we recorded neuronal activity of visual GPe neurons after long-term learning of object values. First, monkeys learned reward values of fractal objects in the object-reward association task (Fig. 3A): half of objects were associated with reward (called ‘good objects’) and the other half with no reward (‘bad objects’) (Kim and Hikosaka, 2013; Yasuda et al., 2012). In this way, each monkey experienced many objects (> 80).

The behavioral effect of the object-reward association was tested using a free viewing procedure (Fig. 3B): 4 objects were chosen randomly and presented on the screen, and the monkey looked at them freely (Fig. 3B, left). No reward was delivered during or after the free viewing. While the object-reward association was repeated across days, the monkey gradually developed value-based gaze bias. After long-term learning (> 4 days for each object) the monkey showed a gaze bias toward good objects (Fig. 3B, center), as reported previously (Kim and Hikosaka, 2013; Yasuda et al., 2012). Interestingly, the gaze bias was caused mainly by the shortening of gaze duration on bad objects ($p<0.01$, Student's t-test), rather than the lengthening of gaze duration on good objects (not significant, Student's t-test) (Fig. 3B, right).

To test neuronal responses to fractal objects after the object-reward association learning, the learned objects were presented one at a time with no contingent reward outcome, while the monkey fixated at a central white dot (passive viewing task) (Fig. 3C). Fig. 3D shows activity of an example neuron in GPe. The neuron responded to fractal objects differentially by their previously learned values: clearly inhibited by 4 bad objects (Fig. 3D, left-bottom), but not by 4 good objects (Fig. 3D, left-top). We tested 2 sets of 8 objects (total: 16 objects) and the neuron's average responses are shown in Figure 3D, right. Both good and bad objects initially induced a transient inhibition, but a more prolonged and stronger inhibition occurred only in response to bad objects (Fig. 3D, right). Therefore, this GPe neuron encoded stable object values.

After the recording of the GPe neuron, we made two electric marking lesions: 1) upper: the border between putamen and GPe (which was estimated electrophysiologically), 2) lower: the recording site of the GPe neuron. These marking lesions were later visualized in a histological section (Fig. 3E), which indicates that the recording site was located in cvGPe where axon terminals of CDt neurons were densely clustered (Fig. 3E, right, see also Fig. 1D).

We examined all visual neurons in GPe (n = 212) using the passive viewing task to test if they encoded stable object values. Among them, 84 neurons were differentially modulated by good and bad objects ($p < 0.05$, Wilcoxon rank-sum test) (Fig. 4A, shown in gray). They were divided into two groups: 1) higher activity with good objects than bad objects (positive-coding), 2) higher activity with bad objects than good objects (negative-coding). Overall, positive-coding neurons (n=62, 74%) were more common than negative-coding neurons (n=22, 26%) (Fig. 4A and B). The population response of all visual neurons in GPe thus showed a clear inhibition to bad objects (Fig. 4C).

These stable value-coding neurons were mainly localized in the caudal-ventral region of GPe (cvGPe) (Fig. 4D) that receives inputs from CDt densely and locally (Fig. 1F and a marking lesion in Fig. 3E). These physiological and anatomical data suggest that CDt-cvGPe connection is activated mainly by stably bad objects, which we will discuss later.

In previous studies, we found that reward values of visual objects can be encoded neuronally and behaviorally in two different manners: flexible or stable (Kim and Hikosaka, 2013). We so far have described stable value coding of GPe neurons. We next tested whether visual

neurons in GPe (n=136) encoded stable and/or flexible values. To examine the flexible value coding, we used flexible value task (Fig. S2A): one of two objects was associated with a reward and the other was not, and the object-reward contingency was reversed in the next block of trials. Among the 134 neurons, only 15 neurons encoded the flexible value positively or negatively ($p < 0.05$, Wilcoxon rank-sum test) (Fig. S2B, gray area, and S2C). Notably, most of stable value-coding neurons were insensitive to flexible values (28 out of 33 neurons, 84.8%) (Fig. 4E).

Convergence of indirect and direct pathways in cdlSNr

We have shown that cvGPe is the first station of the CDt-indirect pathway. However, cvGPe is unlikely to be an output station of the basal ganglia. To understand the CDt-indirect pathway, we need to identify the target of cvGPe. To address this question, we injected CTB555 at the recording site of a stable value-coding neuron, which was in cvGPe (Fig. 5A and D). Anterogradely labeled axon terminals were found in the dorsallateral region of the substantia nigra pars reticulata (SNr) (Fig. 5B) which was located in the caudal region of SNr (Fig. 5C). Thus, cvGPe projects selectively to the caudal-dorsallateral region of SNr (cdlSNr). Since SNr is known to be one of the output stations of the basal ganglia, CDt-cvGPe-cdlSNr circuit would constitute a particular indirect pathway.

This raises an important question: Do the indirect and direct pathways originating from the same region of the striatum (i.e., CDt) converge to the same output region of the basal ganglia? To answer this question, we injected CTB555 in CDt in another monkey (Fig. 5D and E). Anterogradely labeled axon terminals were localized in cdlSNr (Fig. 5F,G and S1B,C,E). These results suggest that CDt targets cdlSNr by both direct and indirect pathways.

Double inhibitory connections in CDt-cvGPe-cdlSNr indirect pathway

cdlSNr is the main output of the basal ganglia that projects to the superior colliculus (Yasuda and Hikosaka, 2015) (SC) and controls saccadic eye movements (Hikosaka and Wurtz, 1983). Therefore, CDt may be able to control saccades using two mechanisms (i.e., direct and indirect pathways to cdlSNr). How do these mechanisms work? Do they process the same or different kinds of information? Do they work cooperatively or competitively? To address these questions, we first electrophysiologically identified neurons that mediate information through the CDt-indirect pathway and then examined the information carried by these neurons.

We first electrically stimulated CDt while recording single neuronal activity in cvGPe (Fig. 6A, top). Among 28 neurons tested, 20 neurons in cvGPe were inhibited (Fig. 6B and Fig. S3). During the passive viewing task, these CDt-inhibited cvGPe neurons, overall, were more inhibited by bad objects than good objects (Fig. 6C). This value bias was statistically significant in 12 out of 20 neurons; the opposite value bias was absent ($p < 0.05$, Wilcoxon rank-sum test) (Fig. 6D). This suggests that CDt mainly sends information on bad objects to cvGPe, which inhibits cvGPe neurons.

We then electrically stimulated cvGPe while recording neuronal activity in cdlSNr (Fig. 6A, bottom). This caused inhibition of cdlSNr neurons (n = 13) (Fig. 6E and S4). During the

passive viewing task, these cvGPe-inhibited cdlSNr neurons, overall, were more excited by bad objects than good objects (Fig. 6F). This value bias was statistically significant in 6 out of 13 neurons; the opposite value bias was absent ($p < 0.05$, Wilcoxon rank-sum test) (Fig. 6G).

These data provide important information about the mechanism and function of the CDt-indirect pathway. First, CDt-cvGPe connection and cvGPe-cdlSNr connection are both inhibitory, and therefore the overall effect of this indirect pathway is disinhibitory (or facilitatory) (Fig. 6A). Second, neurons along the CDt-indirect pathway encode stable values of visual objects, but their response polarities are flipped at each step, due to the inhibitory connections: Bad objects induce inhibitions in cvGPe neurons, which are reversed to excitations in cdlSNr neurons.

GPe-SNr connection for indirect pathway output

We so far have used orthodromic stimulation. This method can examine the signal recipient (e.g., what signal does the cdlSNr neuron receive from cvGPe?), but cannot identify the signal sender. This latter question can be answered by antidromic stimulation. We applied this method for cvGPe-cdlSNr connection, especially because the orthodromic effect might be mediated by another brain area (e.g., subthalamic nucleus).

We thus identified neurons in cvGPe that sent signals to cdlSNr directly (i.e., signal sender) by antidromically activating the cvGPe neuron by stimulating cdlSNr (Fig. 7A). Figure 7B shows an example of antidromically activated neuron in cvGPe. The antidromic response was confirmed by its fixed latency (0.6 ms) (Fig. 7B, top) and collision with spontaneous spikes (Fig. 7B, bottom).

We found 10 antidromically activated neurons in cvGPe. Their antidromic latencies ranged from 0.6 to 0.72 ms (mean latency: 0.66 ± 0.04 ms, mean ± SD). Most of the cdlSNr-projecting cvGPe neurons (6 out of 10) encoded significantly positive values ($p < 0.05$, Wilcoxon rank-sum test) (Fig. 7C): stronger inhibition to bad objects than good objects (Fig. 7D, left). Some of the cdlSNr-projecting cvGPe neurons (2 out of 10) encoded significantly negative values: stronger excitation to bad objects than good objects (Fig. 7D, right).

These results based on electrophysiological and behavioral experiments suggest that CDt-indirect pathway send mainly low-value signals to cdlSNr neurons through two serial inhibitory connections. This would facilitate (i.e., disinhibit) cdlSNr neurons and then inhibit SC neurons, thus suppressing saccades to bad objects (i.e., rejection of valueless objects).

Discussion

Individual parts of our anatomical data (Fig. 1 and 5) are consistent with previous anatomical studies: CDt-cdlSNr and CDt-cvGPe connections in monkeys (Saint-Cyr et al., 1990; Szabo, 1972); GPe-SNr connection in rats (Smith and Bolam, 1989, 1991). Yet, these data together led to an important conclusion: the direct and indirect pathways originating from CDt, both, project to a restricted region of SNr (cdlSNr) (Fig. 8). In addition, our physiological data raise a conceptual hypothesis. A majority of neurons in all of these areas

(CDt, cdlSNr, cvGPe) responded to visual objects, usually with contralateral preferences. While we previously reported visual neurons in CDt (Yamamoto et al., 2012) and cdlSNr (Yasuda et al., 2012), the fact that GPe contains visual neurons is consistent with a previous study (Shin and Sommer, 2010). These visual signals are likely to originate from temporal cortical areas which project to CDt (Saint-Cyr et al., 1990; Yeterian and Pandya, 1995), but other circuits, including one from SC (Ichinohe and Shoumura, 1998; McHaffie et al., 2005; Takada et al., 1985), may be involved. It has been known that a majority of neurons in cdlSNr in monkeys project mostly to the intermediate layer of SC (Yasuda and Hikosaka, 2015) that controls saccadic eye movements (Hikosaka and Wurtz, 1983). Indeed, electrical stimulation of CDt induces saccades with low thresholds, their vectors corresponding to the receptive fields of nearby CDt neurons (Yamamoto et al., 2012). These data suggest that the CDt-direct/indirect pathways contribute to the same single behavior —guiding animals' gaze.

This leads to a next question: which objects do animals look at? There are various reasons to look at particular objects, such as visual salience, multisensory integration, novelty, unexpectedness, etc (Ghazizadeh et al., 2016a; Henderson, 2003; Land et al., 1999; Yarbus et al., 1967). Our data indicate that CDt-direct/indirect pathways focus on another reason: reward value. Importantly, this is 'historical value', not 'expected value': the value of an object is gradually acquired during the long-past experiences of the object in association with a small or large reward, and remains stably fixed with no further reward association (Kim and Hikosaka, 2013; Yamamoto et al., 2013; Yasuda et al., 2012). After experiencing many objects with biased rewards, CDt-direct/indirect pathways continue to encode reward values of many visual objects (Kim and Hikosaka, 2013; Yamamoto et al., 2013).

Here is an important question: how do the direct and indirect pathways work together to 'look at valuable objects'? The major effect of CDt-direct pathway (i.e., CDt-cdlSNr-SC) should be 'disinhibition' because both CDt-cdlSNr and cdlSNr-SC connections are GABAergic inhibitory while cdlSNr neurons are tonically active (Hikosaka and Wurtz, 1983; Smith et al., 1998). If CDt neurons directly projecting to cdlSNr are selectively excited by historically high-valued (good) objects, they would disinhibit SC neurons and facilitate saccades to the good objects (Fig. 8). This was actually found in the cdlSNr-SC connection (Yasuda and Hikosaka, 2015; Yasuda et al., 2012). Why then is CDt-indirect pathway necessary?

Our data show that CDt-indirect pathway consists of three serial inhibitory connections (Fig. 8): CDt-cvGPe (Fig. 6B), cvGPe-cdlSNr (Fig. 6E and 7), cdlSNr-SC (Yasuda and Hikosaka, 2015). A critical part of this circuit (GPe-SNr-SC) has been shown in the rat (Smith and Bolam, 1989, 1991). Almost all neurons along this pathway in the monkey respond to visual fractal objects, and a majority of them encoded historical values. Importantly, many of these neurons were more responsive to low-valued (bad) objects: inhibitions in cvGPe neurons (Fig. 4C and 6C) and excitations (i.e., disinhibitions) in cdlSNr neurons (Fig. 6F). These results suggest that CDt neurons projecting to cvGPe are more activated by bad objects, while CDt neurons projecting to cdlSNr are more activated by good objects (Fig. 8). Indeed, CDt contains good- and bad-preferring neurons (Kim and Hikosaka, 2013). Therefore, the main effect of CDt-indirect pathway would be to suppress saccades to bad objects. The

indirect pathway is similarly important in rodents (Nishizawa et al., 2012; Sano et al., 2013) and humans (Jahfari et al., 2011). Indeed, this function would be critical for survival, as described below.

In real life, animals and humans are surrounded by many objects, and only a small portion of them may be good (e.g., rewarding), while many are bad (e.g., useless). Therefore, to choose good objects, animals need to reject bad objects completely. CDt-indirect pathway would be critical because it encodes stable values of as many bad objects as experienced historically and suppresses saccades to any of them.

We observed this directly during free viewing (Fig. 3B). After monkeys experienced many objects, with either a reward (good objects) or no reward (bad objects), for more than 4 days, the duration of gaze on bad objects decreased strongly (compared with the increased gaze durations for good objects). Such an automatic gaze bias is beneficial for goal-directed behavior: when a good object was presented with several bad objects (search task), monkeys often made a single saccade directly to the good object within 150 ms while ignoring bad objects (Ghazizadeh et al., 2016b). Without CDt-indirect pathway, animals' gaze would be distracted by many bad objects before reaching a good object. Animals would then obtain less reward per time and even may lose the reward (e.g., taken by other animals) (Hikosaka et al., 2013).

Note that some detailed features remain unsolved. First, we found that cvGPe-recipient cdlSNr neurons, overall, were excited by bad objects, but not inhibited by good objects (Fig. 6F). On the other hand, our previous study showed that some cdlSNr neurons are inhibited by good objects (Yasuda and Hikosaka, 2015; Yasuda et al., 2012). It is thus possible that individual cdlSNr neurons receive different amounts of inputs from CDt and cvGPe. If so, CDt-direct/indirect pathways might be separated, to some extent, before reaching SC (Fig. 8). Second, a typical scheme of the indirect pathway is that the connection from GPe to SNr/GPi is mediated by the subthalamic nucleus (STN) (Albin et al., 1989), but our data suggest that cdlSNr receives robust inhibitory inputs directly from cvGPe. In fact, several anatomical studies revealed massive connections from GPe to SNr (Bolam and Smith, 1992; Sato et al., 2000; Smith and Bolam, 1991). However, this does not exclude the possibility that STN is involved in CDt-indirect pathway. In fact, some cvGPe neurons along CDt-indirect pathway were excited by visual objects (Fig. 7D), which may be caused by excitatory inputs from STN (Nambu et al., 2000). Third, while most CDt-recipient cvGPe neurons encoded stable values (Fig. 6D), many other visual neurons in cvGPe showed no value coding (Fig. 4D). These visual neurons might control the baseline threshold of saccades which is unrelated to object values. Finally, the value-coding difference between the direct and indirect pathways, which we found, may not be common across different sets of direct/indirect pathways originating from different regions in the striatum (François et al., 2004; Kelly and Strick, 2004; Lehericy et al., 2006). They may operate in different contexts (Sippy et al., 2015; Tecuapetla et al., 2014; Vicente et al., 2016).

STAR Methods

CONTACT FOR REAGENT AND RESOURCE SHARING

Further information and requests for resources and reagents should be directed to and will be fulfilled by the Lead Contacts Hyoung F. Kim (hyoung.f.kim@gmail.com).

EXPERIMENTAL MODEL AND SUBJECT DETAILS

Animal model

Macaca mulatta: Five adult male monkeys (*Macaca mulatta*, 8–14 years old, male), ZO (9 kg) and AX (9 kg) for neuronal recording and histology, DW (11 kg) and SH (10 kg) for neuronal recording and SM (10 kg) for histology, were used in the experiments. All animal care and experimental procedures were approved by the National Eye Institute Animal Care and Use Committee and complied with the Public Health Service Policy on the humane care and use of laboratory animals.

MTEHOD DETAILS

General procedures—We implanted a plastic head holder and plastic recording chambers to the skull under general anesthesia and sterile surgical conditions. One chamber aiming at GPe and CDt was tilted laterally by 25°, and another chamber aiming at GPe and SNr was tilted posteriorly by 40°. Two search coils were surgically implanted under the conjunctiva of the eyes to record eye movements. After the monkeys fully recovered from surgery, we started training them with object value learning and passive viewing task.

Single unit recording—While the monkey was performing a task, activity of single neurons in target regions was recorded using conventional methods. The recording sites were determined with 1 mm spacing grid system, with the aid of MR images (4.7 T, Bruker) obtained along the direction of the chamber. Single-unit recording was performed using glass-coated electrode (Alpha-Omega). The electrode was inserted into the brain through a stainless-steel guide tube and advanced by an oil-driven micromanipulator (MO-97A, Narishige). The electric signals from the electrode were amplified and band-pass filtered (0.2–10 kHz; BAK). Neuronal spikes were isolated online using a custom voltage-time window discrimination software (MEX, Laboratory or Sensorimotor Research, National Eye Institute-National Institutes of Health [LSR/NEI/NIH] or BLIP, available at www.simonhong.org) and their timings were detected at 1 kHz. The waveforms of individual spikes were collected at 50 kHz.

Behavioral procedure—Behavioral procedures were controlled by QNX-based real-time experimentation data acquisition system (REX, LSR/NEI/NIH) or BLIP. The monkey sat in a primate chair, facing a frontoparallel screen in a sound-attenuated and electrically shielded room. Visual stimuli generated by an active matrix liquid crystal display projector (PJ550, ViewSonic) were rear projected on the screen. We created the visual stimuli using fractal geometry (Yamamoto et al., 2012). Their sizes were ~8°×8°.

The main behavioral procedure consisted of two phases: learning (object-value learning task) and testing (passive viewing task for neuronal testing, free viewing procedure for

behavioral testing). It is important to note that the learning was guided by reward (i.e. water), but the testing was done with no reward outcome. Details are explained below.

Object-value learning task (Fig. 3A)—The purpose of this task was to generate stable value memories by associating visual objects with consistent reward outcomes. A set of eight computer-generated fractal objects was used as visual objects in each session of this and the following tasks. While the monkey was gazing at a central white dot, one of the objects was presented at right or left position pseudorandomly (15° from center). The center spot turned off 400 ms later, and the monkey was required to make a saccade to the objects. Half of the objects were associated with a liquid reward (good objects), whereas the other half were associated with smaller amount of liquid reward or no reward (bad objects). The reward was delivered 600 ms after monkeys held their gaze on the object. One training session consisted of 112 trials (14 trials for each object). Each set was learned in one learning session in one-day. The same sets of objects were repeatedly learned with the same value associations over 4 days. When the neuronal activity was tested, there were more than 80 fractal objects which were learned over 4 days.

Free viewing procedure (Fig. 3B)—To test the behavioral response of the monkey to the value-learned objects, we used a task in which no instruction was required while the learned fractal objects were presented. After the monkey fixated on a central white dot for 300 ms, four objects were chosen pseudorandomly and presented simultaneously in four symmetric positions (15° from center). The monkey was free to gaze at them for 2 s without any reward outcome. To maintain the monkey's motivation, a reward-associated white dot was presented at one of eight positions on half of the trials. If the monkeys made a saccade to it and held the gaze on it for 600 ms, a reward was delivered. Each object was presented at least 16 times in one session.

Passive viewing task (Fig. 3C)—This task was used to examine how the neurons encoded previously learned values of objects without congruent reward outcome. While the monkey was fixating on a central white dot, some of the learned fractal objects (2–6 at once) were sequentially presented at neurons' preferred position. The duration of each object presentation was 400 ms. Reward was independent from the object presentation: it was delivered 300 ms after the last object was presented. The value-coding activity was tested after long-term learning with a sufficient retention period (> 1 day). For each neuron, we used multiple sets of well-learned objects (more than two sets, or 16 objects) to test its stable value-coding during retention.

Flexible value task (Fig. S2A)—To examine neuronal responses in flexible value condition, object-value contingency was reversed in every block of 28–35 trials. Two fractal objects were used as the saccade target. In each trial, one of them was presented at a right or left position pseudorandomly (15° from center). In a block, one of the objects was associated with a liquid reward and the other with no reward or small amount of reward. The reward was delivered 600 ms after monkeys held their gaze on the object. In the next block, the object-reward contingency was reversed.

Spatial preference mapping task—We tested spatial preferences of neurons using spatial mapping task in which an object was presented at 33 different positions. The task procedure was the same as the passive viewing task except for the various object positions. First, the most responsive object was chosen for each neuron using the passive viewing task and used in the spatial mapping task. In each trial the selected object was presented at one position among 33 combinations of 5 eccentricities (0°, 5°, 10°, 20°, 30°) and 8 directions (right, up-right, up, up-left, left, down-left, down, down-right). The object was presented at one of the 33 positions more than 3 times. To examine the contralateral-ipsilateral spatial selectivity, the object was presented at two positions (10 or 15 deg to right and left).

Orthodromic stimulation—To examine physiological effects along the indirect pathway, we inserted two electrodes in 1) CDt and cvGPe (through lateral and posterior chambers, respectively) or 2) cvGPe and cdlSNr (posterior and lateral chambers) (Fig. 6A). To determine the stimulation site, we first identified CDt or cvGPe by the electrophysiological properties (e.g., spike shape, firing rate, firing pattern) and the sensory properties (especially, visual responses) of recorded neurons. When neurons were found that responded to fractal objects with stable values, we fixed the position of the electrode for electrical stimulation. We then lowered the other electrode to cvGPe or cdlSNr for electrical recording. When a stable value-coding neuron was found, we examined its response to the electrical stimulation with the other electrode. For stimulation we used a biphasic pulse (cathodal-anodal, each 0.2 ms duration). The currents for cathodal pulse ranged from 10 to 100 μA (anodal pulse, lower).

Antidromic stimulation—To test if a cvGPe neuron directly projects to cdlSNr, two electrodes were inserted in cvGPe (for recording) and cdlSNr (for stimulation) through the posterior and lateral chambers, respectively (Fig. 7A). When stable value-coding neurons were found in cdlSNr, we fixed the position of the electrode for electrical stimulation. We then lowered the other electrode to cvGPe while stimulating cdSNr repeatedly (about 1 Hz), until we found spikes that were evoked with a fixed latency. The antidromic nature of the spikes was confirmed by a collision test. For stimulation we used a biphasic pulse (cathodal-anodal, each 0.2 ms duration). The currents for cathodal pulse ranged from 20 to 80 μA (anodal pulse, lower).

Tracer injection (Fig. 1)—Before injecting the tracers we identified the injection sites by single unit recording with behavioral tasks (Kim et al., 2014). We used a custom-made injectrode consisting of an epoxy-coated tungsten microelectrode (FHC) for neuron recording and a silica tube (outer/inner tip diameter: 155/75 μm; Polymicro technologies) for tracer injection. A 10-μL Hamilton syringe held in a manual infusion pump (Stoelting) was used to inject 0.3 μl CTB 555 and 0.3 μl CTB 488 (1% in 0.01M, pH 7.4, phosphate buffer) at a speed of 0.01 μl/min. After the injection, the injectrode was left for 1 h to minimize tracer diffusion along the injectrode track.

Histology—Monkeys were deeply anesthetized with an overdose of sodium pentobarbital two weeks after the tracer injection. Saline and 4% paraformaldehyde were perfused transcardially. The head was fixed to the stereotaxic frame, and the brain was cut into blocks

in the coronal plane including basal ganglia structures. The block was post-fixed overnight at 4°C, and then cryoprotected for 5 days in increasing gradients of glycerol solution (5, 10 to 20% in PBS) before being frozen. The frozen block was cut every 50 μm using a microtome. Every 250 μm-interval slices were used for cell counting, and the adjacent slice was used for Nissl staining.

Electric marking lesion—To confirm the locations of cvGPe neurons, we passed a 13 μA-negative current for 30 s after recording of a stable value neuron. The recording site was detected in a Nissl-stained section.

QUANTIFICATION AND STATISTICAL ANALYSIS

Visual response—To examine the neuron's visual response, we counted the numbers of spikes within test and control windows for each fractal object in the passive viewing task (Test window: 50–400 ms after the object onset, Control window: 400–0 ms before the object onset).

To test if the neuron was visually responsive, we compared the numbers of spikes between the control and test windows in individual trials for each object (Fig. 2). To test if the neuron was sensitive to the stable values of objects, we compared its responses to good and bad objects (using more than # objects in each group) (Figs. 4, 6, 7). In both cases, the statistical significance was examined using Wilcoxon rank-sum test. To examine the degree of the value coding, we computed the area under the receiver operating characteristic (ROC) based on the response magnitudes of the neurons to good objects versus bad objects.

Firing irregularity index—To measure irregularity of firing pattern, we calculated an irregularity index (IR index). First, interspike intervals (ISI) between spike i and spike i − 1 (ISI_i), and spike i + 1 and spike i (ISI_{i+1}) were computed. Second, the difference between adjacent ISIs was computed by $| \log(ISI_i/ISI_{i+1}) |$. We then computed a median of all IR values during the inter-trial interval. The small values of IR index indicate regular firing, and large IR index indicates irregular firing (Fig. 2G).

Flexible value coding—To test if the neuron was sensitive to the flexible values of objects, we analyzed the data in the flexible value task and compared its responses to the currently high-valued object and the currently low-valued object (Fig. S2).

Free viewing behavior—To examine the effect of stable object values on the monkey's behavior, we used the free viewing procedure, and measured saccade-choice rate and gaze duration (Fig. 3B). The saccade-choice rate was defined as follows: (nSACg − nSACb)/(nSACg + nSACb) where nSACh and nSACl are the numbers of saccades toward good and bad objects, respectively. The gaze duration was averaged separately for good and bad objects.

DATA AND SOFTWARE AVAILABILITY

The custom codes will be provided upon request to the Lead Contact.

Supplementary Material

Refer to Web version on PubMed Central for supplementary material.

Acknowledgments

We thank D. Parker, I. Bunea, M.K. Smith, G.Tansey, A.M. Nichols, T.W. Ruffner, J.W. McClurkin, and A.V. Hays for technical assistance. This research was supported by the Intramural Research Program at the National Institutes of Health, National Eye Institute and IBS-R015-D1.

References

Albin RL, Young AB, Penney JB. The functional anatomy of basal ganglia disorders. Trends Neurosci. 1989; 12:366–375. [PubMed: 2479133]

Alexander GE, Crutcher MD. Functional architecture of basal ganglia circuits: neural substrates of parallel processing. Trends Neurosci. 1990; 13:266–271. [PubMed: 1695401]

Bolam JP, Smith Y. The striatum and the globus pallidus send convergent synaptic inputs onto single cells in the entopeduncular nucleus of the rat: a double anterograde labelling study combined with postembedding immunocytochemistry for GABA. J Comp Neurol. 1992; 321:456–476. [PubMed: 1380517]

Cui G, Jun SB, Jin X, Pham MD, Vogel SS, Lovinger DM, Costa RM. Concurrent activation of striatal direct and indirect pathways during action initiation. Nature. 2013; 494:238–242. [PubMed: 23354054]

François C, Grabli D, McCairn K, Jan C, Karachi C, Hirsch EC, Féger J, Tremblay L. Behavioural disorders induced by external globus pallidus dysfunction in primates II. Anatomical study Brain. 2004; 127:2055–2070. [PubMed: 15292054]

Ghazizadeh A, Griggs W, Hikosaka O. Ecological origins of object salience: Reward, uncertainty, aversiveness, and novelty. Front Neurosci. 2016a; 10:1–16. [PubMed: 26858586]

Ghazizadeh A, Griggs W, Hikosaka O. Object-finding skill created by repeated reward experience. J Vis. 2016b; 16:17.

Graybiel AM. Neurotransmitters and neuromodulators in the basal ganglia. Trends Neurosci. 1990; 13:244–254. [PubMed: 1695398]

Henderson JM. Human gaze control during real-world scene perception. Trends Cogn Sci. 2003; 7:498–504. [PubMed: 14585447]

Hikida T, Kimura K, Wada N, Funabiki K, Nakanishi S. Distinct roles of synaptic transmission in direct and indirect striatal pathways to reward and aversive behavior. Neuron. 2010; 66:896–907. [PubMed: 20620875]

Hikosaka O, Wurtz RH. Visual and oculomotor functions of monkey substantia nigra pars reticulata. IV. Relation of substantia nigra to superior colliculus. J Neurophysiol. 1983; 49:1285–1301. [PubMed: 6306173]

Hikosaka O, Takikawa Y, Kawagoe R. Role of the basal ganglia in the control of purposive saccadic eye movements. Physiol Rev. 2000; 80:953–978. [PubMed: 10893428]

Hikosaka O, Yamamoto S, Yasuda M, Kim HF. Why skill matters. Trends Cogn Sci. 2013; 17:434–441. [PubMed: 23911579]

Hikosaka O, Kim HF, Yasuda M, Yamamoto S. Basal Ganglia circuits for reward value-guided behavior. Annu Rview Neurosci. 2014; 37:289–306.

Ichinohe N, Shoumura K. A di-synaptic projection from the superior colliculus to the head of the caudate nucleus via the centromedian-parafascicular complex in the cat: An anterograde and retrograde labeling study. Neurosci Res. 1998; 32:295–303. [PubMed: 9950056]

Jahfari S, Waldorp L, van den Wildenberg WP, Scholte HS, Ridderinkhof KR, Forstmann BU. Effective Connectivity Reveals Important Roles for Both the Hyperdirect (Fronto-Subthalamic) and the Indirect (Fronto-Striatal-Pallidal) Fronto-Basal Ganglia Pathways during Response Inhibition. J Neurosci. 2011; 31:6891–6899. [PubMed: 21543619]

Kelly RM, Strick PL. Macro-architecture of basal ganglia loops with the cerebral cortex: use of rabies virus to reveal multisynaptic circuits. Prog Brain Res. 2004; 143:449–459. [PubMed: 14653187]

Kim HF, Hikosaka O. Distinct Basal Ganglia circuits controlling behaviors guided by flexible and stable values. Neuron. 2013; 79:1001–1010. [PubMed: 23954031]

Kim HF, Ghazizadeh A, Hikosaka O. Separate groups of dopamine neurons innervate caudate head and tail encoding flexible and stable value memories. Front Neuroanat. 2014; 8:120. [PubMed: 25400553]

Kita H. GABAergic circuits of the striatum. Prog Brain Res. 1993; 99:51–72. [PubMed: 8108557]

Kravitz AV, Freeze BS, Parker PRL, Kay K, Thwin MT, Deisseroth K, Kreitzer AC. Regulation of parkinsonian motor behaviours by optogenetic control of basal ganglia circuitry. Nature. 2010; 466:622–626. [PubMed: 20613723]

Kravitz AV, Tye LD, Kreitzer AC. Distinct roles for direct and indirect pathway striatal neurons in reinforcement. Nat Neurosci. 2012; 15:816–818. [PubMed: 22544310]

Land M, Mennie N, Rusted J. The roles of vision and eye movements in the control of activities of daily living. Perception. 1999; 28:1311–1328. [PubMed: 10755142]

Lehericy S, Bardinet E, Tremblay L, Van de Moortele PF, Pochon JB, Dormont D, Kim DS, Yelnik J, Ugurbil K. Motor control in basal ganglia circuits using fMRI and brain atlas approaches. Cereb Cortex. 2006; 16:149–161. [PubMed: 15858164]

Lévesque M, Parent A. The striatofugal fiber system in primates: a reevaluation of its organization based on single-axon tracing studies. Proc Natl Acad Sci U S A. 2005; 102:11888–11893. [PubMed: 16087877]

Marsden CD. The mysterious motor function of the basal ganglia: the Robert Wartenberg lecture. Neurology. 1982; 32:514–539. [PubMed: 7200209]

McHaffie JG, Stanford TR, Stein BE, Coizet V, Redgrave P. Subcortical loops through the basal ganglia. Trends Neurosci. 2005; 28:401–407. [PubMed: 15982753]

Nambu A, Tokuno H, Hamada I, Kita H, Imanishi M, Akazawa T, Ikeuchi Y, Hasegawa N. Excitatory cortical inputs to pallidal neurons via the subthalamic nucleus in the monkey. J Neurophysiol. 2000; 84:289–300. [PubMed: 10899204]

Nishizawa K, Fukabori R, Okada K, Kai N, Uchigashima M, Watanabe M, Shiota A, Ueda M, Tsutsui Y, Kobayashi K. Striatal Indirect Pathway Contributes to Selection Accuracy of Learned Motor Actions. J Neurosci. 2012; 32:13421–13432. [PubMed: 23015433]

O'Doherty J, Dayan P, Schultz J, Deichmann R, Friston K, Dolan RJ. Dissociable Role of Ventral and Dorsal Striatum in Instrumental Conditioning. Science. 2004; 304:452–454. [PubMed: 15087550]

Roseberry TK, Lee AM, Lalive AL, Wilbrecht L, Bonci A, Kreitzer AC. Cell-Type-Specific Control of Brainstem Locomotor Circuits by Basal Ganglia. Cell. 2016; 164:526–537. [PubMed: 26824660]

Saint-Cyr JA, Ungerleider LG, Desimone R. Organization of visual cortical inputs to the striatum and subsequent outputs to the pallido-nigral complex in the monkey. J Comp Neurol. 1990; 298:129–156. [PubMed: 1698830]

Samejima K, Ueda Y, Doya K, Kimura M. Representation of action-specific reward values in the striatum. Science. 2005; 310:1337–1340. [PubMed: 16311337]

Sano H, Chiken S, Hikida T, Kobayashi K, Nambu A. Signals through the Striatopallidal Indirect Pathway Stop Movements by Phasic Excitation in the Substantia Nigra. J Neurosci. 2013; 33:7583–7594. [PubMed: 23616563]

Sato F, Lavallée P, Lévesque M, Parent A. Single-axon tracing study of neurons of the external segment of the globus pallidus in primate. J Comp Neurol. 2000; 417:17–31. [PubMed: 10660885]

Schultz W, Dayan P, Montague PR. A neural substrate of prediction and reward. Science. 1997; 275:1593–1599. [PubMed: 9054347]

Shin S, Sommer MA. Activity of neurons in monkey globus pallidus during oculomotor behavior compared with that in substantia nigra pars reticulata. J Neurophysiol. 2010; 103:1874–1887. [PubMed: 20107133]

Sippy T, Lapray D, Crochet S, Petersen CC. Cell-Type-Specific Sensorimotor Processing in Striatal Projection Neurons during Goal-Directed Behavior. Neuron. 2015; 88:298–305. [PubMed: 26439527]

Smith Y, Bolam JP. Neurons of the substantia nigra reticulata receive a dense GABA-containing input from the globus pallidus in the rat. Brain Res. 1989; 493:160–167. [PubMed: 2476197]

Smith Y, Bolam JP. Convergence of synaptic inputs from the striatum and the globus pallidus onto identified nigrocollicular cells in the rat: a double anterograde labelling study. Neuroscience. 1991; 44:45–73. [PubMed: 1722893]

Smith Y, Bevan MD, Shink E, Bolam JP. Microcircuitry of the direct and indirect pathways of the basal ganglia. Neuroscience. 1998; 86:353–387. [PubMed: 9881853]

Szabo J. The Course and Distribution of Tail of the Caudate Nucleus Efferents from in the Monkey the. Exp Neurol. 1972; 572:562–572.

Tai LH, Lee AM, Benavidez N, Bonci A, Wilbrecht L. Transient stimulation of distinct subpopulations of striatal neurons mimics changes in action value. Nat Neurosci. 2012; 15:1281–1289. [PubMed: 22902719]

Takada M, Itoh K, Yasui Y, Sugimoto T, Mizuno N. Topographical projections from the posterior thalamic regions to the striatum in the cat, with reference to possible tecto-thalamo-striatal connections. Exp Brain Res. 1985; 60:385–396. [PubMed: 4054280]

Tecuapetla F, Matias S, Dugue GP, Mainen ZF, Costa RM. Balanced activity in basal ganglia projection pathways is critical for contraversive movements. Nat Commun. 2014; 5:4315. [PubMed: 25002180]

Vicente AM, Galvao-Ferreira P, Tecuapetla F, Costa RM. Direct and indirect dorsolateral striatum pathways reinforce different action strategies. Curr Biol. 2016; 26:R267–9. [PubMed: 27046807]

Yamamoto S, Monosov IE, Yasuda M, Hikosaka O. What and where information in the caudate tail guides saccades to visual objects. J Neurosci. 2012; 32:11005–11016. [PubMed: 22875934]

Yamamoto S, Kim HF, Hikosaka O. Reward value-contingent changes of visual responses in the primate caudate tail associated with a visuomotor skill. J Neurosci. 2013; 33:11227–11238. [PubMed: 23825426]

Yarbus A, Haigh B, Rigss L. Eye Movements and Vision. 1967

Yasuda M, Hikosaka O. Functional territories in primate substantia nigra pars reticulata separately signaling stable and flexible values. J Neurophysiol. 2015; 113:1681–1696. [PubMed: 25540224]

Yasuda M, Yamamoto S, Hikosaka O. Robust Representation of Stable Object Values in the Oculomotor Basal Ganglia. J Neurosci. 2012; 32:16917–16932. [PubMed: 23175843]

Yeterian EH, Pandya DN. Corticostriatal connections of extrastriate visual areas in rhesus monkeys. J Comp Neurol. 1995; 352:436–457. [PubMed: 7706560]

Yoshida M, Precht W. Monosynaptic inhibition of neurons of the substantia nigra by caudatonigral fibers. Brain Res. 1971; 32:225–228. [PubMed: 4329651]

Highlights

-Direct and indirect pathways of caudate tail encode object values in opposite manners.

-They both control saccades by sending opposite value signals to superior colliculus.

-Both value signals are mediated by serial point-to-point inhibitory connections.

-These pathways together can guide good object choice and bad object rejection.

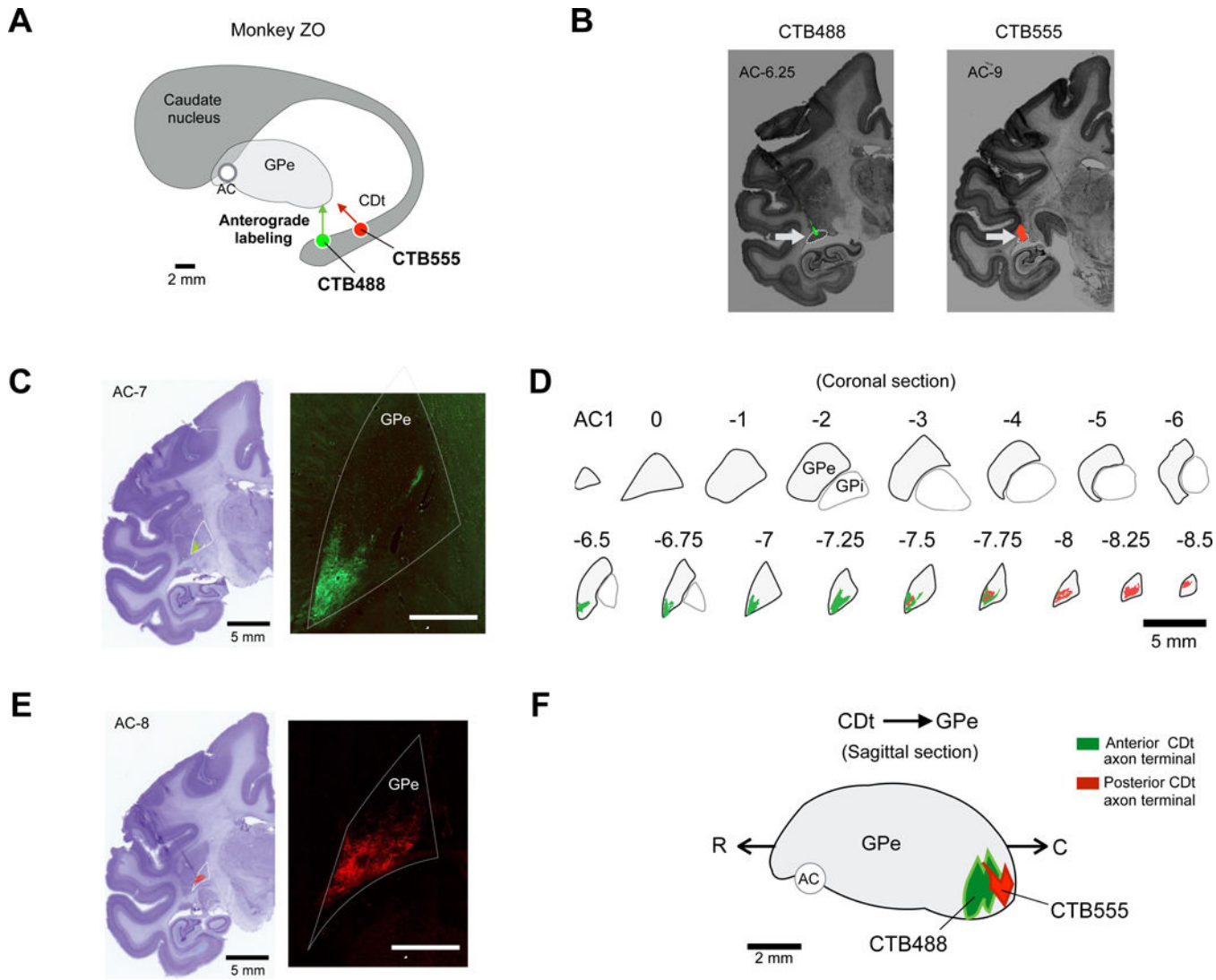

Figure 1. CDt projection to caudal-ventral region of GPe

(A) Scheme of injection sites in CDt in monkey ZO. CTB488 and CTB555 were injected in anterior and posterior regions of CDt respectively. **(B)** Injection sites in the anterior and posterior CDt. Fluorescent signals were detected in each region of CDt (White arrows). **(C and E)** Examples of axon terminal signals in GPe. Axonal plexus (green and red signals) were detected in coronal slices of GPe. White bar: 5 mm **(D)** CDt projection sites in coronal slices of GPe. Axon terminals of CDt neurons were mainly found in caudal-ventral regions of GPe (cvGPe). **(F)** Sagittal view of CDt-projection site in GPe. CTB555 and CTB488 signals were topographically organized in rostral-caudal axis of GPe.

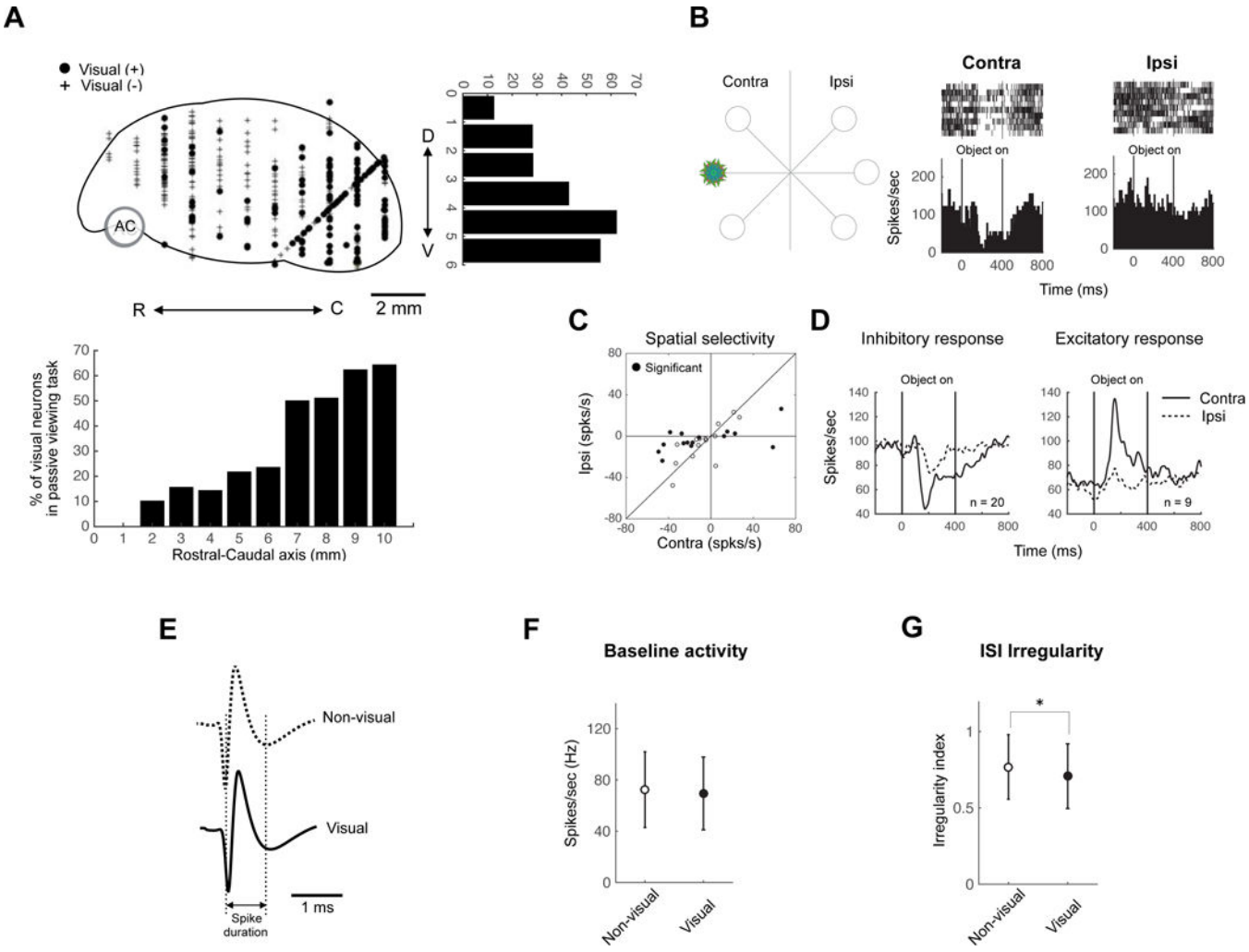

Figure 2. Visual neurons in GPe

(A) Locations of visually responsive neurons in sagittal view. D, dorsal; V, ventral; R, rostral; C, caudal. Neuronal distributions are projected to rostral-caudal axis (down) and dorsal-ventral axis (right). Number 0 indicates the rostral and dorsal ends of GPe. **(B)** An example visual response of GPe neuron. One object was presented in contralateral and ipsilateral hemifields to the recording site (left). The example neuron showed inhibitory response to the object presented in contralateral field (middle) but no response to the same one presented in ipsilateral field (right). **(C)** Comparison between the responses to contralateral objects (abscissa) and ipsilateral objects (ordinate) for individual neurons. The response was determined by the change in activity from the baseline period (−400–0 ms before object presentation) to the test period (50–400 ms after object presentation). **(D)** Population response of two types of visual neurons. Average neuronal responses (shown by peristimulus time histogram [PSTH]) are aligned on the time of object presentation (0–400 ms). **(E–G)** Electrophysiological properties of visual and non-visual neurons in GPe. Visual and non-visual neurons had similar spike shapes **(E)** and baseline activity **(F)**. However visual GPe neuron had lower inter-trial-interval irregularity than non-visual neurons **(G)** (mean ± SD, * $p < 0.05$).

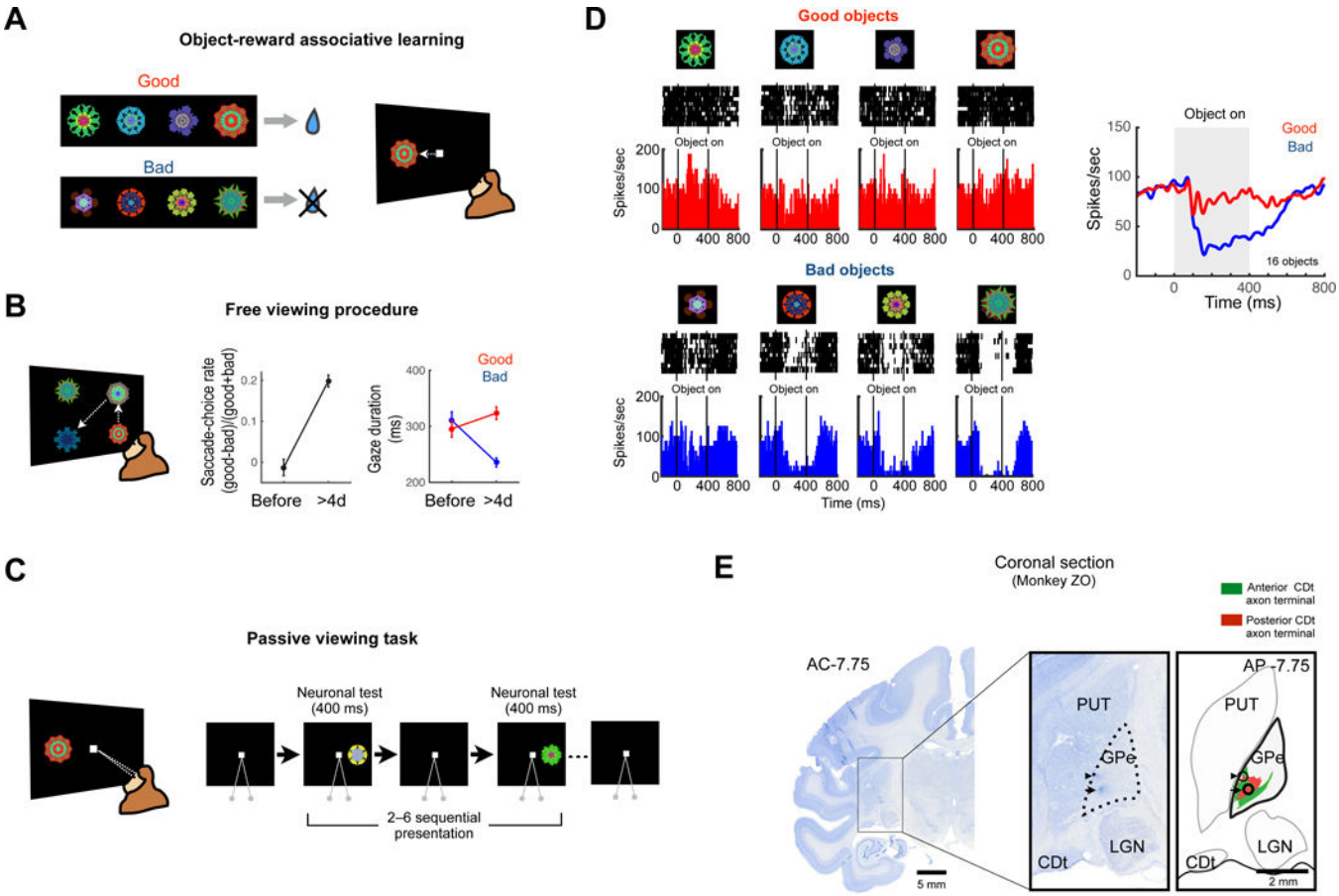

Figure 3. Stable value coding for habitual behavior in cvGPe

(A) Object-reward associative learning. An example set of fractal objects that were associated with stable values. During long-term learning, the half of objects were associated with a reward (good objects), while the other objects were associated with no reward (bad objects). **(B)** Free viewing procedure for testing habitual gaze to previously learned objects. Four of eight objects in one set (as in A) was presented, and the monkey freely looked at it without direct reward outcome. After long-term learning (> 4-day) and more than one-day retention, the monkeys showed gaze preference for the good objects (mean ± SE). **(C)** Passive viewing task to test neuronal response to learned objects. While the monkey fixated at a central white dot, two to six fractal objects were pseudorandomly chosen from a set of eight objects and were sequentially presented in the neurons' preferred location. **(D)** An example GPe neuron encoding stable object value. Shown are its responses to eight long-term learned objects (left) and the average responses to good objects (red) and bad objects (blue) (right). **(E)** Location of a stable value-coding neuron in GPe, indicated by a marking lesion (black arrow) in a Nissl-stained coronal section. Another marking lesion was made 1 mm above the neuron (black arrowhead). The marking lesions were located in the CDt projection area shown in Figure 1D (right).

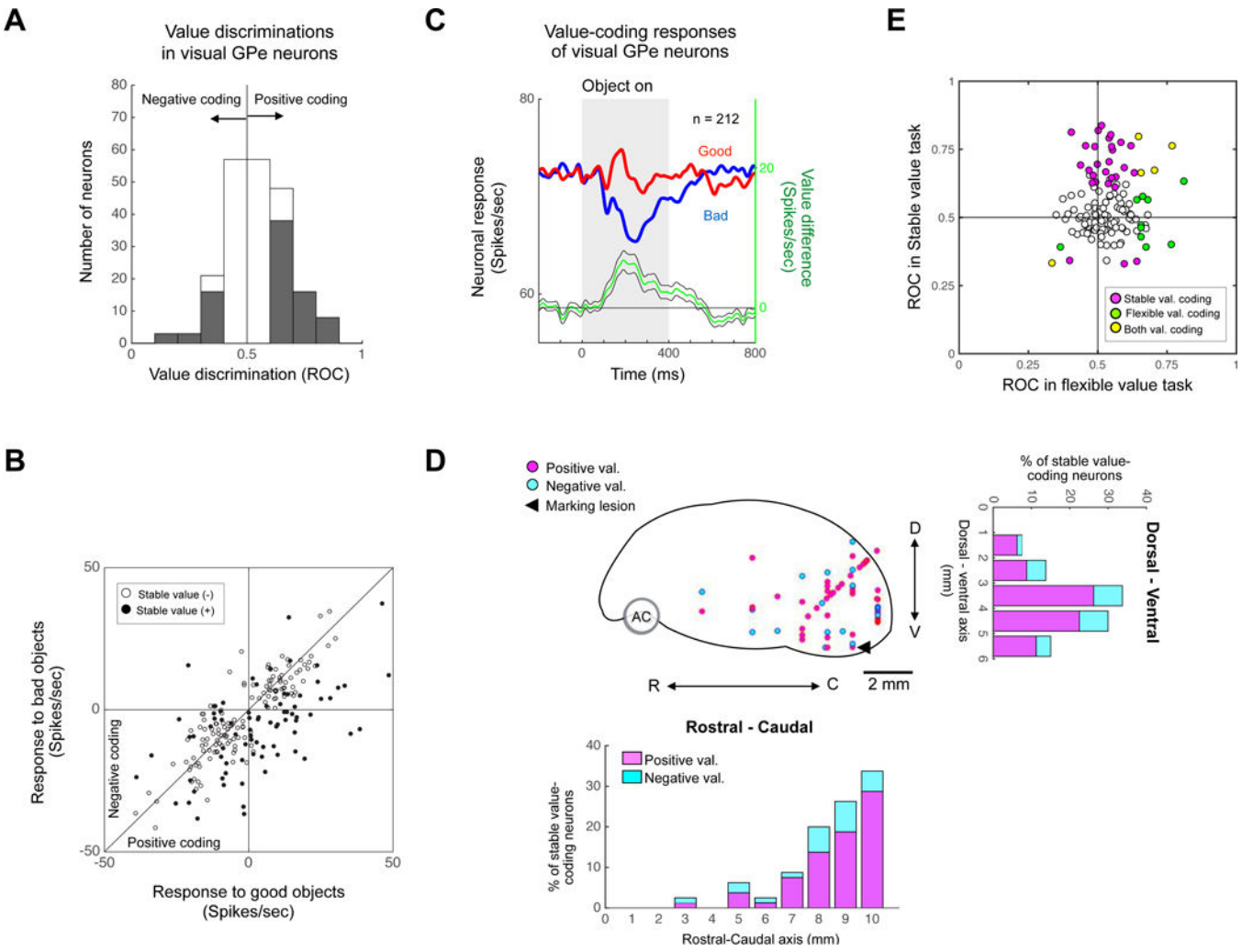

Figure 4. Population activity of stable value coding in GPe

(A) Stable value discrimination of visual GPe neurons. For each neuron, the difference in response to good and bad objects was calculated as ROC area. ROC > 0.5: Good > Bad, ROC < 0.5: Bad > Good. Gray area indicates neurons that showed statistically significant stable value coding. **(B)** Comparison between responses to good objects (abscissa) and bad objects (ordinate) in passive viewing task for visual GPe neurons. The response was determined by the change in activity from the baseline to test period (as in Figure 2C). **(C)** Population response of visual GPe neurons to learned objects in passive viewing task. Green line indicates the value coding (i.e., good – bad) (mean ± SE). **(D)** Locations of stable value-coding neurons in sagittal view. D, dorsal; V, ventral; R, rostral; C, caudal. Neuronal distributions are projected to rostral-caudal axis (down) and dorsal-ventral axis (right). Number 0 indicates the rostral or dorsal border of GP. **(E)** Comparison between response to flexible (abscissa) and stable (ordinate) value coding for individual neurons. ROCs indicate the value discrimination calculated with neuronal responses in passive viewing task (Fig. 3C) and flexible value task (Fig. S2A).

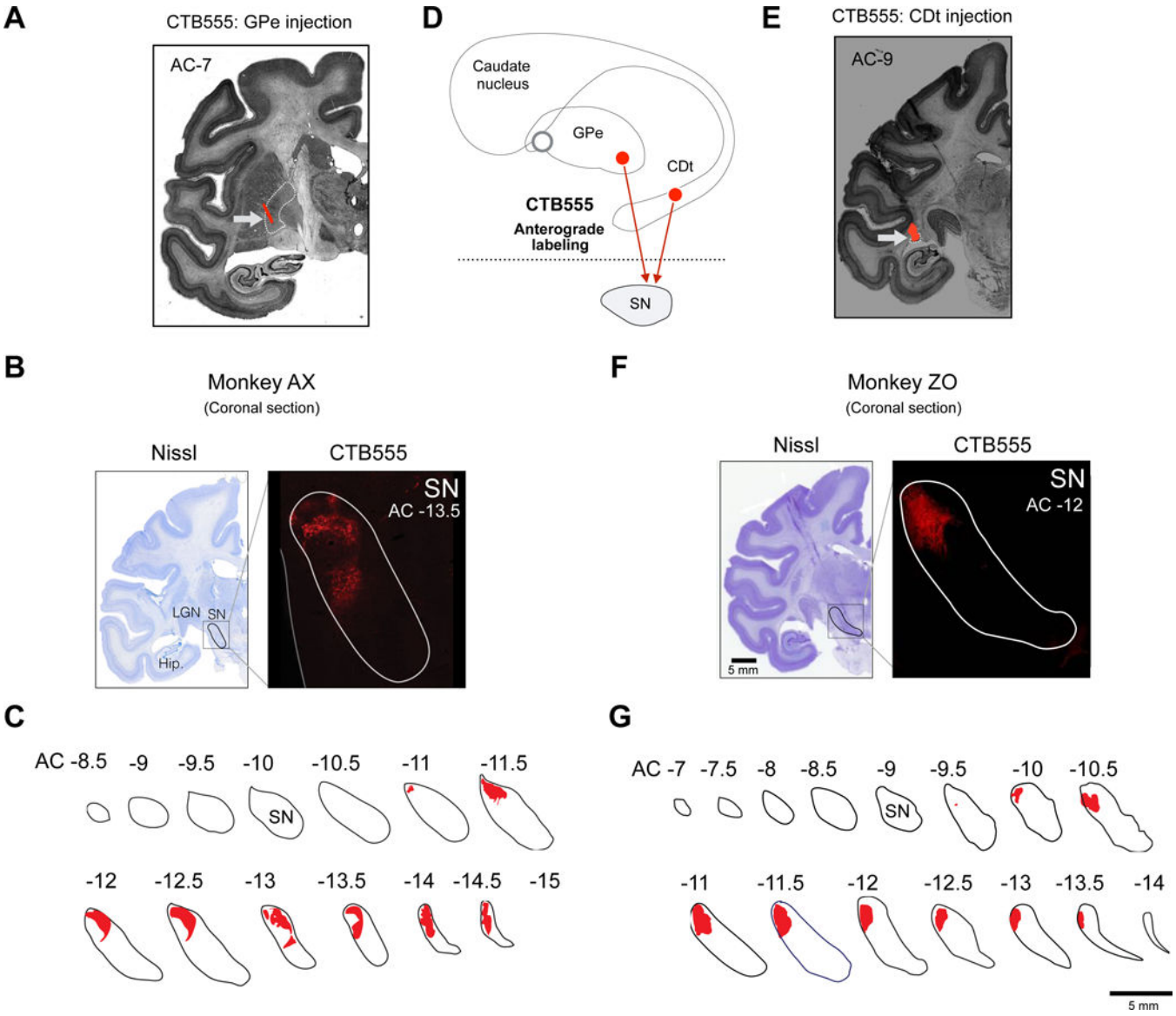

Figure 5. Convergence of direct and indirect pathways in cdlSNr

(A) Tracer injection site in cvGP in monkey AX. CTB555 was injected while single unit recording of stable value-coding GPe neuron, and the injection site was found in cvGPe (white arrow). **(B)** An example slice of cvGPe projection site in SNr. Axon terminal labeled by CTB555 (red) was found in lateral region of SN. **(C)** GPe projection sites in coronal slices of SNr. Axon terminals of CDt neurons were mainly found in caudal-dorsal-lateral region of SNr (cdlSNr). **(D)** Scheme of injection sites in cvGPe and CDt. CTB555 was injected in cvGPe or CDt of different monkeys. **(E)** Injection site in CDt in monkey ZO. CTB555 signal was indicated by white arrow. **(F)** An example slice of CDt projection site in SNr. CTB555 signal (red) was also detected in lateral region of SN. **(G)** CDt projection sites in coronal slices of SNr. Axon terminals of CDt neurons were found in caudal-dorsal-ventral region of SNr (cdlSNr).

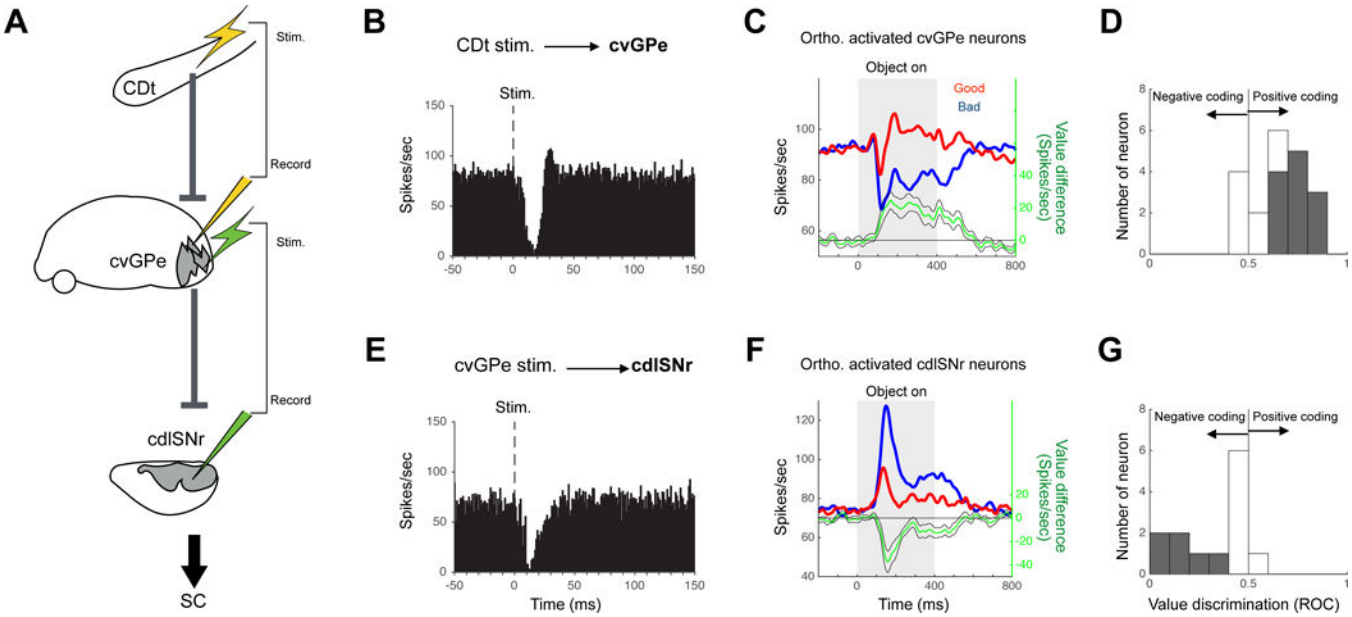

Figure 6. Double inhibitions and flipped value coding in CDt-cvGPe-cdlSNr indirect pathway

(A) Experiment to study the orthodromic stimulation effects along the indirect pathway. CDt, caudate tail. cvGPe, caudal-ventral globus pallidus external segment. cdlSNr, caudal-dorsal-lateral substantia nigra pars reticulata. **(B)** Orthodromic responses of cvGPe neurons by CDt stimulation. Average activity of 20 neurons. **(C–D)** Stable value discrimination of the orthodromically responsive GPe neurons. **(C)** Population response (same format as Fig. 4C). **(D)** Value discrimination of individual neurons (same format as Fig. 4A). **(E)** Orthodromic responses of cdlSNr neurons by cvGPe stimulation. Average activity of 13 neurons. **(F–G)** Stable value discrimination of the orthodromically responsive cdlSNr neurons.

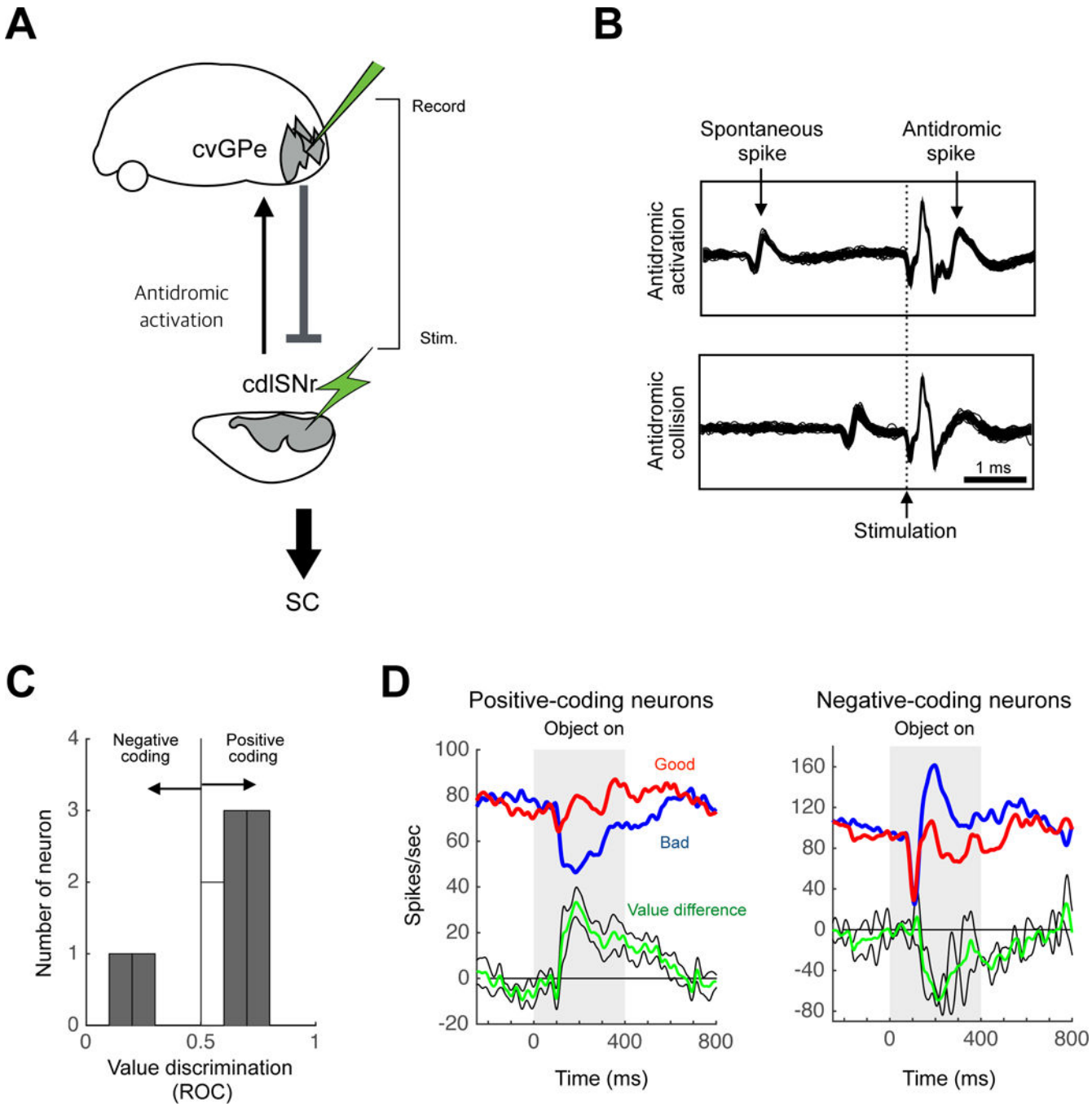

Figure 7. Stable value-coding cvGPe neurons project to cdlSNr directly

(A) Experiment to study the antidromic stimulation effects for the cvGPe-cdlSNr connection. **(B)** A cvGPe neuron activated antidromically by electrical stimulation in cdlSNr with a fixed latency of 0.6 ms (top). This activation was eliminated when CDt stimulation occurred within 1.06 ms after a spontaneous spike (bottom), confirming its antidromic nature (collision test). **(C–D)** Stable value discrimination of the antidromically responsive cvGPe neurons. **(C)** Value discrimination of individual neurons. **(D)** Population responses,

shown separately for positive-coding neurons (left, n=6) and negative-coding neurons (right, n=2).

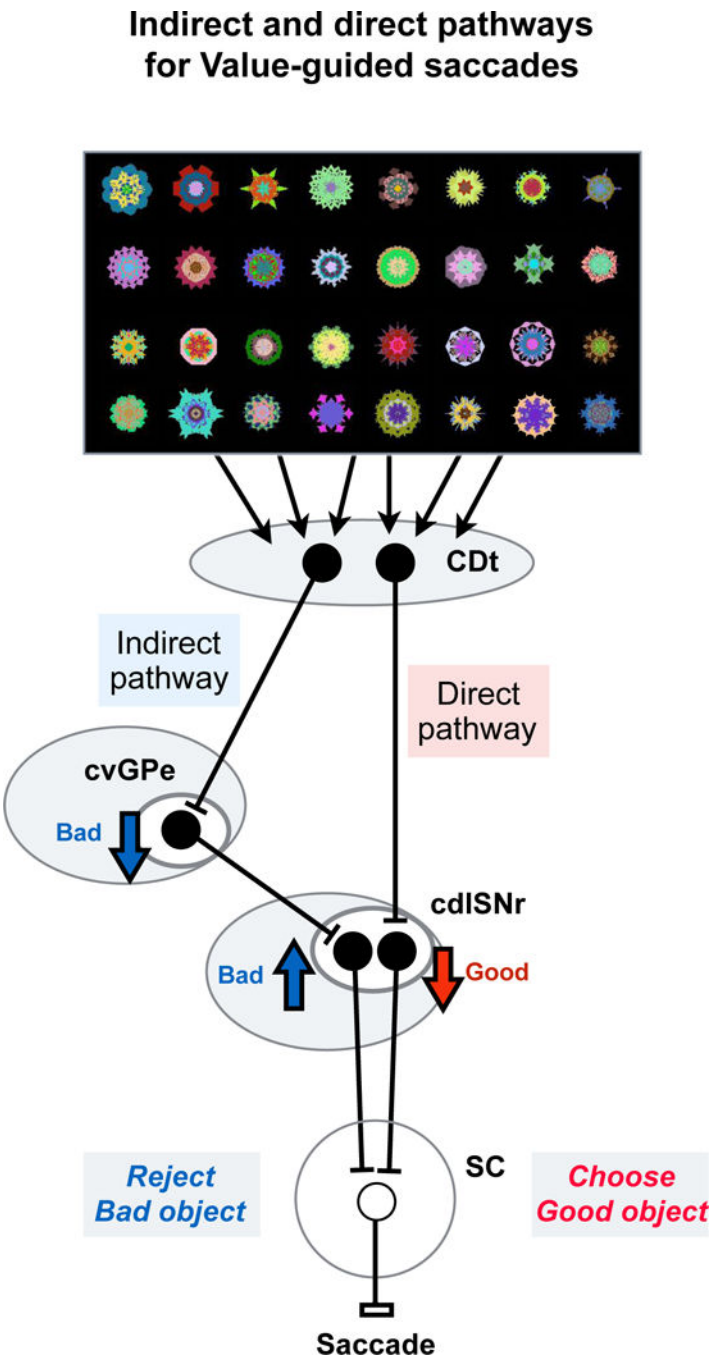

Figure 8. Direct and indirect pathways to determine the goal of saccadic eye movement

Differential information processing through direct and indirect pathways. In this scheme, inhibitory and excitatory neurons are shown by black and white circles. CDt neurons process visual objects selectively, together with their positions and stable reward values(Kim and Hikosaka, 2013; Yamamoto et al., 2013). This set of information is then processed through its direct pathway (CDt-cdlSNr) and indirect pathway (CDt-cvGPe-cdlSNr). Both pathways are sensitive to stable (not flexible) reward values of visual objects, but in opposite manners: direct pathway sensitive to good (historically high-valued) objects, indirect pathway

sensitive to bad (historically low-valued) objects. The information on good objects leads to a disinhibition of saccadic neurons in SC (through the direct pathway), facilitating saccades to good objects. The information on bad objects leads to an enhanced inhibition of saccadic neurons in SC (through the indirect pathway), suppressing saccades to bad objects.